Taylor & Francis
Taylor & Francis Group

Check for updates

RESEARCH PAPER

miR-208b modulating skeletal muscle development and energy homoeostasis through targeting distinct targets

Liangliang Fu[a,b], Heng Wang[a,b], Yinlong Liao[a,b], Peng Zhou[a,b], Yueyuan Xu[a,b], Yunxia Zhao[a,b], Shengsong Xie[a,b], Shuhong Zhao[a,b], and Xinyun Li[a,b]

[a]Key Laboratory of Agricultural Animal Genetics, Breeding, and Reproduction of the Ministry of Education & Key Laboratory of Swine Genetics and Breeding of Ministry of Agriculture, Huazhong Agricultural University, Wuhan, P. R. China; [b]The Cooperative Innovation Center for Sustainable Pig Production, Wuhan, P. R. China

ABSTRACT

Embryonic and neonatal skeletal muscles grow via the proliferation and fusion of myogenic cells, whereas adult skeletal muscle adapts largely by remodelling pre-existing myofibers and optimizing metabolic balance. It has been reported that miRNAs played key roles during skeletal muscle development through targeting different genes at post-transcriptional level. In this study, we show that a single miRNA (miR-208b) can modulate both the myogenesis and homoeostasis of skeletal muscle by distinct targets. As results, miR-208b accelerates the proliferation and inhibits the differentiation of myogenic cells by targeting the E-protein family member transcription factor 12 (TCF12). Also, miR-208b can stimulate fast-to-slow fibre conversion and oxidative metabolism programme through targeting folliculin interacting protein 1 (FNIP1) but not TCF12 gene. Further, miR-208b could active the AMPK/PGC-1a signalling and mitochondrial biogenesis through targeting FNIP1. Thus, miR-208b could mediate skeletal muscle development and homoeostasis through specifically targeting of TCF12 and FNIP1.

Introduction

Skeletal muscle is the largest organ in mammals, which plays vital roles in mobility and metabolism [1]. During development, massive proliferation and fusion of myogenic cells are necessary to construct hundreds of muscle pieces throughout the body [2,3,]. In the adult skeletal muscle, consistent remodelling of contractile myofiber composition and energy utilization and endocrine responses occurs throughout life, dysfunction of muscle development leads to a variety of muscle disease, such as Duchenne muscular dystrophy (DMD) in humans [4–6].

In addition, skeletal muscle tissue of livestock is the major source of protein for humans. Therefore, uncovering the molecular mechanism of skeletal muscle development is essential for both human health and animal production. MicroRNAs (miRNAs) are key regulators in skeletal muscle development. It has been reported that some muscle enriched miRNAs play important roles in muscle development, including skeletal and cardiac-muscle-specific miR-206, miR-1, and miR-133, as well as ubiquitously expressed miRNAs, such as miR-29, miR-378, miR-497/195, and miR-431 [7–12]. Many important factors of muscle development, including PAX3, PAX7, MyoD, MyoG, MSTN, and IGF1R, are regulated by those miRNAs in muscle development [13–16]. Some miRNAs have also been reported to have several targets during tissue development. However, few studies have confirmed that miRNA could play different roles in targeting different genes in muscle development.

Three miRNAs are located at the intron of myosin genes. miR-208a is located at the intron of MYH6, which is specifically expressed in the cardiac tissue. miR-208b is located at the intron of MYH7, which is specifically expressed in skeletal muscle after birth; it is also expressed in cardiac muscle at embryonic stages [17]. miR-499 is located at the intron of Myh7b, which is expressed in both cardiac and skeletal muscles [17]. In zebrafish, Sox6 gene is targeted by both miR-208b and miR-499, which plays important roles in muscle fibre confirmation [18]. Overexpression of miR-499 could partially rescue the symptom of Duchenne muscular dystrophy (DMD) by increasing mitochondrial oxidative metabolism [19]. Interestingly, previous studies indicate that the roles of the miR-208a and miR-499 are opposite in the regulation of energy metabolism [20,21,]. However, the roles of miR-208b in myogenesis and energy metabolism still remain largely unknown.

In this study, we focused on the muscle-specific miR-208b and systematically analysed its targets and the signalling pathways responsible for skeletal muscle development. We showed that this miRNA could efficiently regulate different biological processes. miR-208b could balance the proliferation and differentiation of myogenic cells through inhibiting TCF12. FNIP1 was recruited and targeted by the miR-208b to control the muscle fibre type composition and energy metabolism.

Thus, miR-208b mediated skeletal muscle development and homoeostasis by targeting distinct genes.

Results

miR-208b inhibits skeletal muscle growth at postnatal

To examine the roles of miR-208b in skeletal muscle, we first constructed miR-208b conditional overexpression mice. The miR-208b skeletal-muscle-specific overexpression TG mice named as Myll-208b were generated through crossing with Myl1-cre and Loxp-miR-208b mice (Supplementary Fig. 1A-C). Q-PCR results showed that miR-208b was only up-regulated significantly in skeletal muscle tissue in Myl1-208b mice compared with those in WT mice (Supplementary Fig. 1D). The Myl1-208b mice have an overall reduction in body weight at 1 month of age (Fig. 1A). The body weight reduction was mainly due to muscle loss, as shown by the significant lighter gastrocnemius (GA) muscles in the Myl1-208b mice (Fig. 1B). To evaluate the skeletal muscle in detail, GA muscles were sectioned and stained with laminin to visualize individual myofibers. Myl1-208b mice had a greatly reduced muscle fibre cross-sectional area (CSA) (Fig. 1C). Specifically, in WT mice, 47.5% of muscle fibres had an area of $\geq 3\,000$ μm^2. However, in the Myl1-208b mice, only 4.8% was found to be of similar diameter (Fig. 1D).

miR-208b promotes proliferation and prevents differentiation of C2C12 myoblasts

The C2C12 myoblasts in vitro differentiation system were used to examine the roles of miR-208b in myogenesis. First, we transfected synthesized miR-208b mimic into C2C12 myoblasts. Then, Q-PCR confirmed that the expression level of miR-208b in cells with miR-208b mimics transfected was significantly higher than that in NC mimics transfected cells (p < 0.01) (Fig. 2E). Further, EdU staining was performed after transfection at 24 h. As results, the EdU positive cells in miR-208b transfected cells were significantly higher than that in mut-miR-208b, or NC controls (P < 0.05) (Fig. 2A–B). Also, fluorescence-activated cell sorting (FACS) showed that a higher percentage of cells in the S phase and a lower percentage in the G1 phase when miR-208b mimics transfected than that in NC control (Fig. 2C). The results indicated that miR-208b overexpression could promote the proliferation of myoblasts.

Further, the roles of miR-208b in the differentiation of myoblast have been studied. MyHc immunostaining results showed that fewer myotubes were generated when miR-208b was overexpressed, and vice versa (Fig. 2D). The activity of creatine kinase (CK) in C2C12 with miR-208b mimic transfected was significantly lower than that in NC mimics transfected group at 72 h after myogenic differentiation (FiG. 2G). Q-PCR results also showed that the expression of MHC, MCK, and MyoG marker
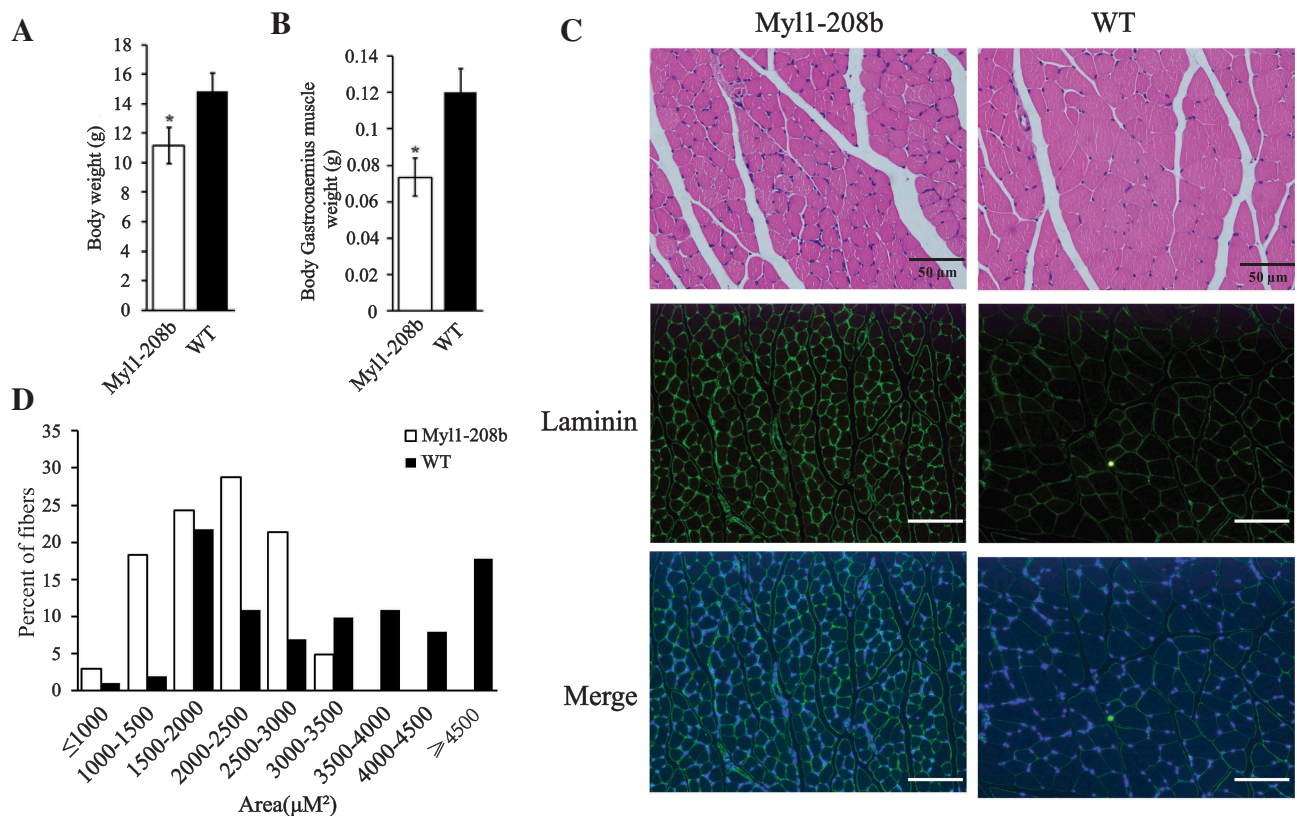

Figure 1. miR-208b inhibits skeletal muscle growth at postnatal.

(A) Body weight (g) and (B) GA (gastrocnemius) muscle weight (g) in WT and Myl1-208b mice at 1 month of age; (C) Immunohistochemistry analysis of GA muscle. Top panel: H&E staining; middle and bottom panel: laminin and DAPI staining. (D) Frequency of distribution for cross-section area (CSA, μm^2) of myofibers from GA muscle. The results are presented as mean ± SEM (n = 3). *, P < 0.05.
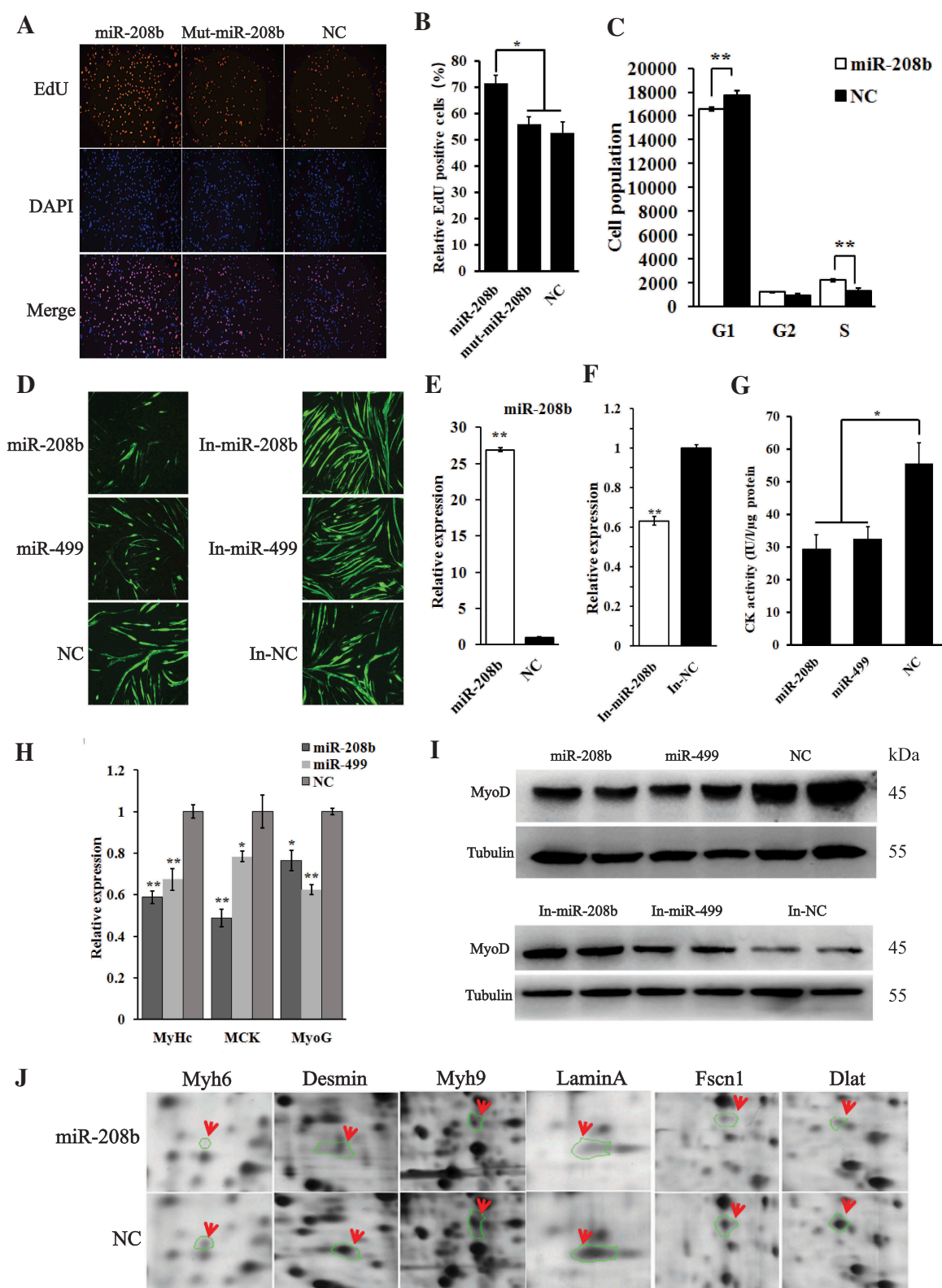
Figure 2. miR-208b promotes C2C12 myoblast proliferation and prevents differentiation.

(A) EdU staining of the proliferating myoblasts after miR-208b overexpression. C2C12 myoblasts were transfected with miR-208b mimic, mut-miR-208b, or control mimics and incubated with EdU for 24 h. Scale bar: 100μm. (B) The percentage of dual positive cells of EdU and DAPI staining. (C) C2C12 cells transfected with miR-208b mimic or NC were collected for cell cycle analysis 24 h after transfection. Cells were stained by propidium iodide and subjected to fluorescence-activated cell sorting analysis by flow cytometry. (D) Representative images showing differentiated myotubes treated with different miRNA mimics or inhibitors. C2C12 myoblast cells were transfected 4 times at 24 h intervals with miRNA-208b, miRNA-499, NC, miRNA-208b inhibitor, miRNA-499 inhibitor, or NC inhibitor. MyHc staining was performed at 5 days of differentiation. Scale bar: 100μm. (E and F) The Q-PCR results of miR-208b in C2C12 cells with miR-208b mimic or inhibitor miR-208b transfected, respectively. (G) The creatine kinase activity at 72 h of C2C12 differentiation when miR-208b or miR-499 overexpressed. (H) Q-PCR analysis of myogenic genes in myotubes treated with different miRNA mimics. (I) Western blotting analysis of MyoD protein level in differentiated myotubes treated with different miRNA mimics or inhibitors. (J) Scan of master gel used for spot comparison and selection. Whole protein preparations were differentially labelled with Cydyes and separated by isoelectric focusing and apparent molecular weight. MYH6, Desmin, Myh9, LaminA, Fscn1 and Dlat1 were down-regulated protein expression in the miR-208b overexpressing myoblasts by mass spectrum analysis. The results are presented as mean ± SEM (n = 3). The mRNA of tubulin was used as internal control for the expression of functional genes. *, P < 0.05; **, P < 0.01.

genes of differentiation was reduced when miR-208b was over-expressed (Fig. 2H). Western blot results showed that MyoD was down-regulated in miR-208b overexpressed myoblasts and was up-regulated in miR-208b inhibited myoblast (Fig. 2F,I). Moreover, MyoD and MyoG were also down-regulated in skeletal muscle tissue of Myl1-208b mice compared to WT mice (Supplementary Fig. 1E). In addition, miR-499 has a similar, yet a little bit weaker effects with miR-208b on myogenic differentiation (Fig. 2D,G–i). The exchange of protein levels in the miR-208b mimics transfected myoblasts was further analysed using 2D electrophoresis and Mass spectra approach. As a result, several muscle structural and cytoskeleton component proteins including LaminA, Desmin, MYH6, and MYH9, were down-regulated when miR-208b was overexpressed (Fig. 2K and Supplementary Table 1). Collectively, the data from both *in vitro* and *in vivo* studies confirmed the pivotal role of miR-208b is balancing cell proliferation and differentiation in skeletal muscle.

miR-208b represses TCF12 during skeletal muscle development

The potential targets of miR-208b were predicted using Targetscan software. One conserved binding site of miR-208b at TCF12 3′-UTR has been found (Supplementary Fig. 2A). Also, transcriptome analysis showed that TCF12 were down-regulated when miR-208b was overexpressed. Thus, TCF12 has been considered as a target of miR-208b. To validate this target, luciferase reporter vectors carrying wild and mutant TCF12 3′-UTR were constructed, respectively. As a result, the luciferase activity of wild TCF12 3′-UTR was significantly reduced when miR-208b, or miR-499 mimics were transfected. However, the luciferase activity has no significant change when Mut-miR-208b, Mut-miR-499 mimics were transfected (Fig. 3A). Furthermore, no change in the mutant TCF12 3′-UTR construction has been observed (Fig. 3B). Biotinylated miR-208b pull-down assays showed that TCF12 mRNA was significantly enriched when biotin-miR-208b was transfected at 0 h and 72 h after differentiation (Fig. 3C). Q-PCR results showed that miR-208b were gradually upregulated, while TCF12 is gradually downregulated during C2C12 differentiation (Fig. 3D,E). Q-PCR and Western blot results showed that both mRNA and protein levels of TCF12 were lower in the miR-208b overexpressed myoblasts (Fig. 3F,G). Also, the protein level of TCF12 increased when miR-208b was inhibited (Fig. 3H). Moreover, TCF12 was down-regulated in the leg skeletal muscle tissue of Myl1-208b mice (FIg. 3I). These results indicated that miR-208b could directly repress TCF12 gene at both mRNA and protein level. The miR-499 could also target TCF12 gene but has relatively weaker effects compared to miR-208b (Fig. 3A,B,G,H).

Further, the transcriptomes of C2C12 cells with miR-208b overexpression and si-TCF12 were analysed. As a result, 1599 and 1454 differentially expressed genes were found in miR-208b mimics and si-TCF12 transfected myoblasts, respectively (Supplementary Table 2). Among them, 656 genes were found in both treatments, which includes key genes of cell cycle and myogenic differentiation (Fig. 3J–L, Supplementary Table 3). KEGG pathway analysis showed that these 656 genes were enriched in key pathways of muscle development which includes muscle contraction; hypertrophic cardiomyopathy,

focal adhesion, etc. (Supplementary Fig. 2B). These data suggested that miR-208b and TCF12 signalling pathways converged during the proliferation and differentiation of muscle cells, thereby further support the idea that TCF12 is a major target of miR-208b in skeletal muscle.

TCF12 is a potent pro-differentiation factor in skeletal muscle

TCF12 has been previously denoted as human basic-helix-loop-helix factor (HEB), which is a member of the E protein family [22]. To study the roles of TCF12 in myogenesis, the interaction of TCF12, MyoD, and MyoG was first analysed. ChIP-seq data analysis results showed that TCF12 together with MyoD and MyoG could bind to the same promoter regions of MyoD and MyoG, especially at differentiation stages (Fig. 4A,B). MyoD and MyoG also bound to the same promoter regions of TCF12 gene, but with no TCF12 binding itself (Fig. 4C). Moreover, Co-IP results showed that TCF12 protein interacted with MyoD and MyoG in myoblasts (Fig. 4D). Furthermore, we combine the results of the TCF12 binding genomic loci and the differentially expressed genes induced by si-TCF12. In total, 747 differentially expressed genes were identified with the TCF12 binding signal, which would be regulated by TCF12 directly (Supplementary Table 4). Notably, all the genes related to myogenic differentiation were down-regulated, while most of the proliferation relative genes were up-regulated (Fig. 4E, supplementary Table 4). GO analysis showed that these genes were enriched in pathways of proliferation and differentiation of myoblast, which including cell cycle, actin cytoskeleton, and hypertrophic cardiomyopathy, etc. (Fig. 4F).

Furthermore, the proliferation ability of myoblast was negatively correlated with the expression level TCF12 based on cell cycle detection (Supplementary Fig. 3A,B). MyHc immunostaining results showed less myotubes were generated during differentiation when TCF12 was inhibited, vice versa (Fig. 4G). However, there was a significant increase in the number of myotubes inferred by the immunofluorescence detection of MyHc when TCF12 was overexpressed (Fig. 4H). Moreover, the activity of CK in C2C12 cells was significantly decreased when TCF12 was inhibited (Supplementary Fig. 3C). Q-PCR showed that the expression level of MyoG and MCK, two differentiation marker genes, was positively correlated with the level of TCF12 (Supplementary Fig. 3D,E). In addition, the rescue assay results showed that the effect of miR-208b on proliferation and differentiation of myoblasts was attenuated when its target TCF12 gene was co-transfected (Supplementary Fig. 3F-H). Therefore, TCF12 was a potent pro-differentiation myogenic factor, which was regulated directly by miR-208b during myogenesis.

miR-208b stimulates fast to slow muscle fibre conversion and mitochondrial energy metabolism

The roles of miR-208b in energy metabolism were studied in GA tissue of 2-month-old Myl1-208b mice. Slow twitch-specific myosin heavy chain 7 (MYH7) staining results showed that Myl1-208b mice contained more type I myofiber compared to wild-type littermates (Fig. 5A).
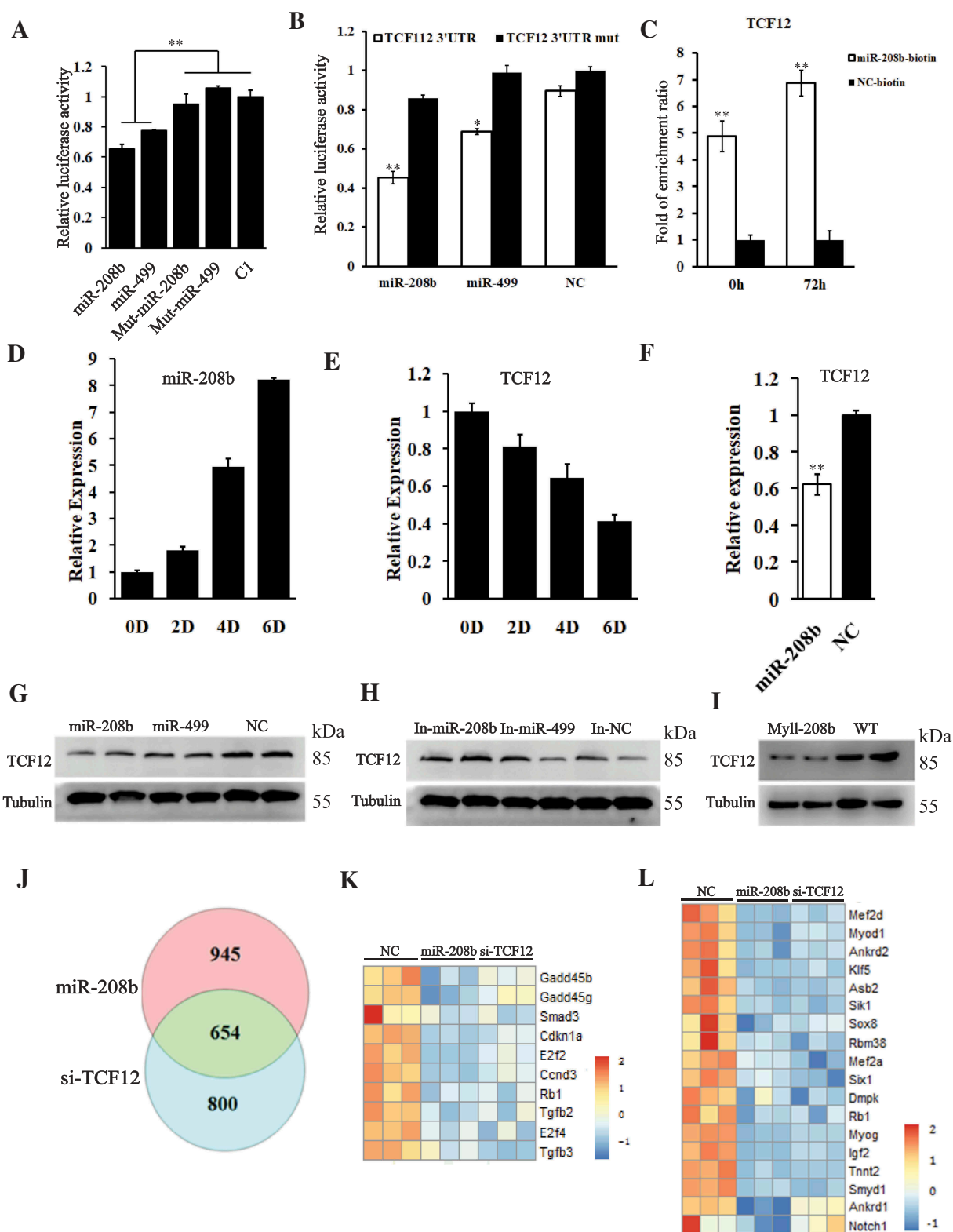
Figure 3. miR-208b represses TCF12 during skeletal muscle development.

(A and B) Wild and mutant TCF12 3′ UTR were inserted into the dual-luciferase reporter vector psi-CHECK2 at the 3′ end of the *Renilla* gene (*hRluc*). Then, the constructs were co-transfected with one of the constructs of pEGFP-miR-208b, pEGFP-mut-miR-208b, pEGFP-miR-499, pEGFP-mut-miR-499, or pEGFP-C1 (C1) into BHK-21 cells. The luciferase activity was analysed after 24 h transfection. (C) The miR-208b-biotin pull-down assays were performed and the TCF12 mRNA level was detected by Q-PCR. (D and E) Q-PCR results of miR-208b and TCF12 during C2C12 differentiation. (F) Q-PCR results of TCF12 in C2C12 cells with or without miR-208b mimics transfection. (G and H) C2C12 myoblast cells transfected with different miRNA mimics or inhibitors miRNA were differentiated for 72 h. TCF12 protein expression was detected by western blotting. (I) The leg muscle protein level of TCF12 was detected in WT and Myl1-208b mice at 1 month of age. (J) A total of 654 genes were identified in the differentially expressed genes from both miR-208b and si-TCF12 transcriptome and was represented by a Venn diagram. (K and L) GO analysis of the 654 common differentially expressed genes indicates significant enrichment of genes involved in negative regulation of cell cycle and myogenic differentiation. The results are presented as mean ± SEM (n = 3). U6 mRNA was used as internal control for miR-208b expression. *, P < 0.05; **P < 0.01.
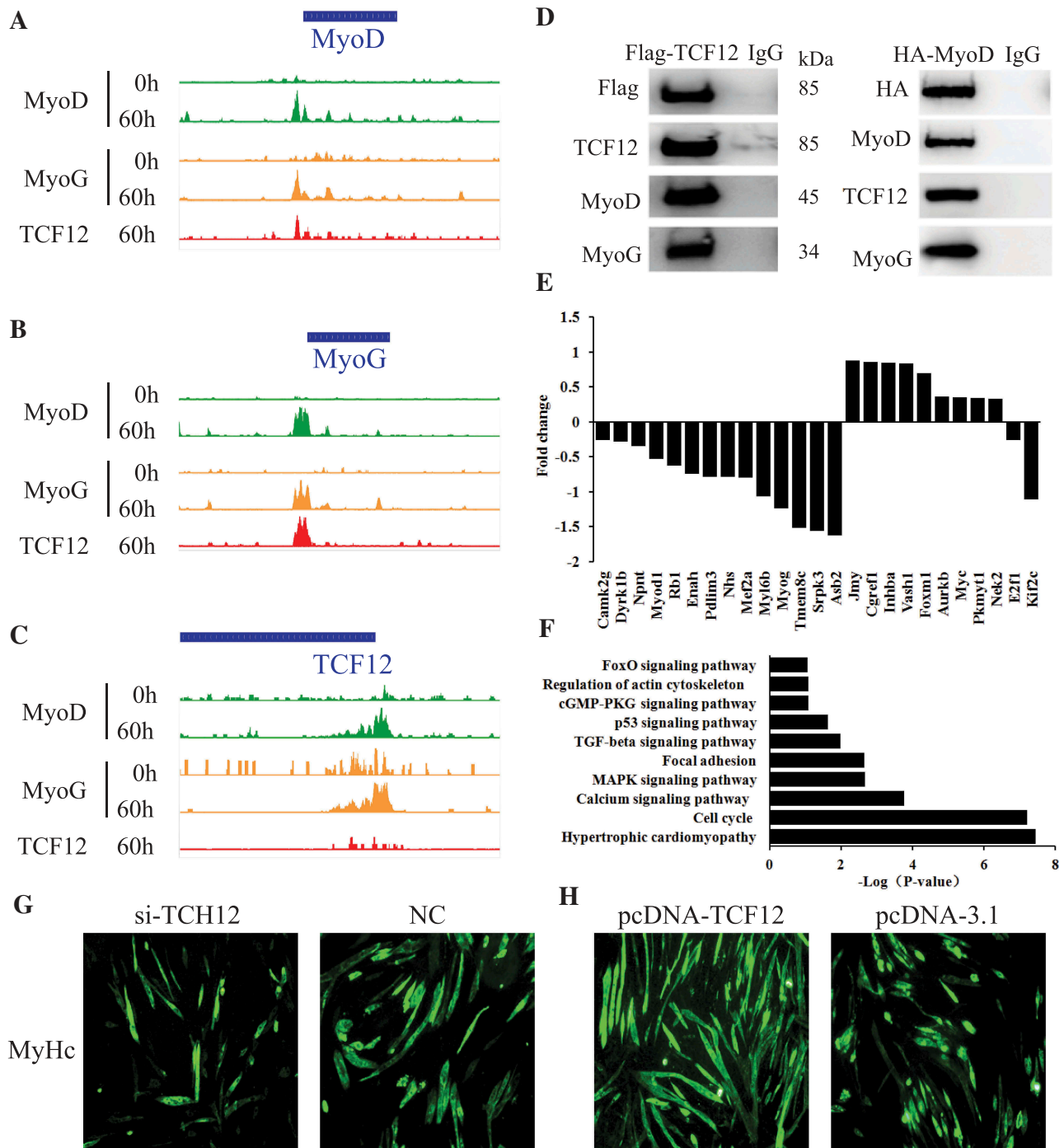
Figure 4. TCF12 is a potent pro-differentiation factor in skeletal muscle.
(A-C) ChIP-seq profile shows the co-localization of MyoD, MyoG, and TCF12 on MyoD, MyoG, and TCF12 loci in C2C12 myoblasts or myotubes. (D) C2C12 cells were transfected with pcDNA-Flag-TCF12 plasmid and pcDNA-HA-myoD, respectively. 72 h after differentiation, cell lysates were subjected to IP. Co-immunoprecipitated proteins of MyoD, MyoG, and TCF12 were detected by western blotting. (E) Combined analysis of the si-TCF12 transcriptome and TCF12 ChIP-seq showed that common differentially expressed genes were mainly involved in cell cycle and myogenesis regulation. (F) KEEG pathway analysis showed that cell cycle, actin cytoskeleton, and hypertrophic cardiomyopathy were enriched. (G and H) Immunofluorescence detection of MyHc (green) in C2C12 cells when TCF12 overexpression (pcDNA-TCF12) or TCF12 knockdown (si-TCF12). NC and pcDNA3.1 used as controls. Scale bar: 100 μm.

Consistent with the fast to slow fibre shift, the electron microscope analysis showed a higher level of mitochondrial number in the Myl1-208b mice than these in control (Fig. 5A). Q-PCR also confirmed the expression of MyHc-I and MyHc-IIa slow fibre markers increased, while the expression of MyHc-IIx fast fibre markers decreased in leg muscle tissue of Myl1-208b mice (Fig. 5B). Also, the expression of mitochondrial energy metabolism genes was up-regulated in leg muscle tissue of Myl1-208b mice (Fig. 5C). These results indicated that miR-208b reprogrammed the muscle tissue for increased mitochondrial oxidative capacity, as well as slow-twitch muscle fibre type *in vivo*.
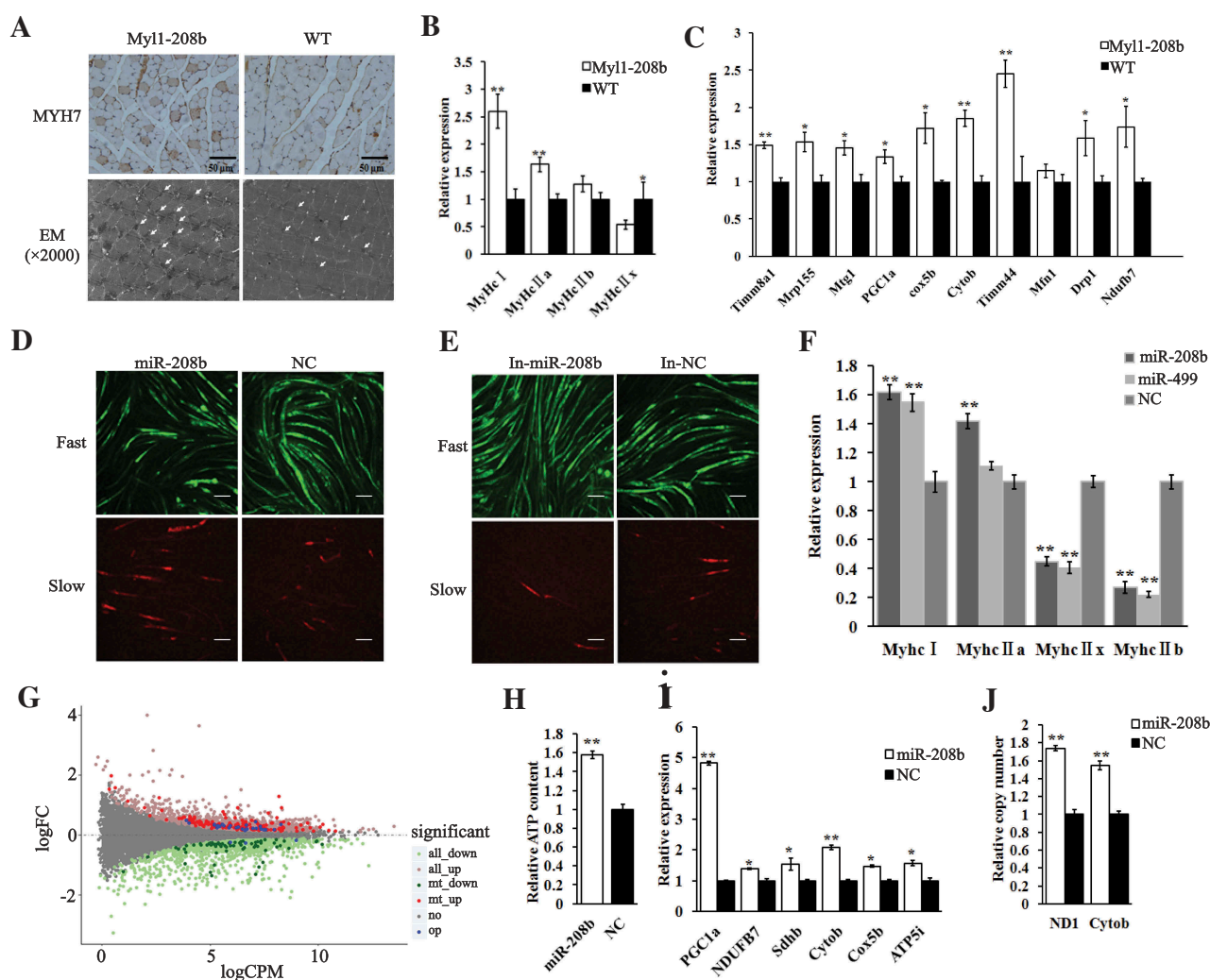
Figure 5. miR-208b stimulates fast to slow muscle fibre conversion and mitochondrial energy metabolism.
(A) Analysis of GA muscle from both miR-208b overexpression and control mice. MYH7 staining showed slow type fibre in cross-sections (top). Scale bar: 200μm. Electron microscope (EM) showing mitochondria distribution (white arrows) in the miR-208b overexpression and control muscles (bottom) Scale bar: 2000μm. (B) The mRNA expression of the MyHc-I, MyHc-IIa, MyHcIIb, and MyHcIIx genes in the leg muscle from WT and Myl1-208b mice at 2 months of age. (C) Genes involved in mitochondria biogenesis were upregulated in Myl1-208b mice. (D and E) C2C12 myoblasts were differentiated into myotubes for 96 h, and myotubes were transfected with miR-208b mimics or miR-208b inhibitor. Immunostaining of C2C12 myotubes was performed using myosin-fast and myosin-slow antibody, respectively. Scale bar: 100μm. (F) C2C12 myotubes were transfected with miR-208b mimic, miR-499 mimic, or NC. The mRNA expression of MyHc-I, MyHc-IIa, MyHcIIb, and MyHcIIx genes was detected by Q-PCR. (G) The MAplot revealed the genes that changed significantly between the miR-208b overexpression and NC. all_down: all the down-regulated genes, all_up: all the up-regulated genes, mt_up: up-regulated mitochondrial genes, mt_up: down-regulated mitochondrial genes, no: no difference gene, op: mitochondrial oxidative phosphorylation genes. (H-J) C2C12 myoblasts were transfected with miR-208b mimic or NC. (H) ATP production; (I) The mRNA expression of mitochondrial energy metabolism genes (PGC1a, NDUFB7, Sdhb, Cytob, Cox5b, and Atp5i) was detected by Q-PCR. (J) The copy number of mitochondria genes (ND1 and Cytob) was detected by Q-PCR. The results are presented as mean ± SEM (n = 3). Tubulin mRNA was used as internal control for the expression of functional genes. *, P < 0.05; **, P < 0.01.

To investigate the underlying mechanisms of miR-208b in regulating muscle fibre type composition, we performed miR-208b loss- or gain-of-function assays in C2C12 myotubes. Immunofluorescence staining showed that miR-208b overexpression could increase the number of myosin-slow positive myotubes and reduce the number of myosin-fast positive myotubes (Fig. 5D). On the contrary, inhibition of miR-208b reduced the slow type but increased the fast type myotubes (Fig. 5E). Q-PCR analysis also showed that overexpression of miR-208b could up-regulate the slow MyHc-I and MyHc-IIa myofiber marker genes in C2C12 myotubes (Fig. 5F). Furthermore, the transcriptome data also showed that genes involved in oxidative phosphorylation and mitochondrial energy metabolism pathway were up-regulated

in miR-208b overexpressed myoblasts (FiG. 5G, Supplementary Table 2). miR-208b overexpression increased the number of mitochondria based on the inflorescence intense of Mito-Tracker (Supplementary Fig. 4A). ATP production was also strengthened in the miR-208b overexpression myoblasts (Fig. 5H). Accordingly, Q-PCR showed that the copy number of mitochondria genes (ND1 and Cytob) and mitochondrial energy metabolism genes (PGC1a, Cytob, and Atp5i) was up-regulated (FIg. 5I,J). Collectively, these *in vitro* data confirmed the role of miR-208b in slow fibre type transition and oxidative energy utilization.

As TCF12 was targeted by miR-208b to control muscle cell proliferation and differentiation, we expected that TCF12 would

also regulate muscle fibre specification. However, we were intrigued by the observation that the overexpression of TCF12 could not alter the muscle fibre type composition (Supplementary Fig. 4B). Furthermore, the GO analysis results showed that no energy metabolism terms were enriched in si-TCF12 myoblast, but they were significantly enriched in miR-208b overexpression myoblast (Supplementary Fig. 4C,D). Therefore, miR-208b regulates energy metabolism and fibre type conversion through TCF12 independent way.

miR-208b regulates energy metabolism and fibre type conversion through targeting FNIP1 gene

In order to study the target genes of miR-208b in energy metabolism and muscle fibre type conversion. Targetscan analysis was performed and a potential conserved miR-208b binding site in the 3′ UTR of the FNIP1 gene was found. The luciferase assay results showed that FNIP1 was targeted by miR-208b (Fig. 6A,B). Biotinylated miR-208b pull-down confirmed that FNIP1 was targeted by miR-208b (Fig. 6C). Moreover, a decrease in FNIP1 mRNA and protein levels was observed in C2C12 myotubes that overexpressed miR-208b, while an increase FNIP1 was observed when miR-208b was inhibited (Fig. 6D–F). FNIP1 protein was also reduced in leg muscle of 2-month-old Myl1-208b mice (FiG. 6G). Therefore, miR-208b directly targets FNIP1. A previous study showed that FNIP1 is involved in the phosphorylation of AMPK, which indicates the vital role of AMPK-PGC1a in energy metabolism signalling pathway [19]. As results, in Myl1-208b mice, protein levels of AMPK, PGC1a, and Cytob increased in leg muscle tissue, which corresponded to the down-regulation of FNIP1 (Fig. 6G). To further verify the roles of FNIP1 in miR-208b mediated muscle fibre type specification and mitochondrial function, FNIP1 knockdown was performed. As expected, the number of type I slow fibres in C2C12 myotubes and the expression of slow fibre genes (MyHc-I and MyHc-IIa) increased, and the opposite remodelling was observed in fast-type fibres genes (MyHc-IIb and MyHc-IIx) (Fig. 6H–I). Furthermore, siRNA knockdown of FNIP1 up-regulated the expression of mitochondrial energy metabolism genes in C2C12 myotubes (Fig. 6J). Moreover, miR-208b could up-regulate PGC1a, Cytob, and p-AMPK but did not affect the total AMPK in C2C12 myotubes (Supplementary Fig. 5A). In addition, the rescue assay results showed that the effect of miR-208b on switch of slow to fast conversion was attenuated when its target FNIP1 gene was co-transfected (Supplementary Fig. 5B–D). Therefore, miR-208b regulated energy metabolism and muscle fibre type conversion through targeting FNIP1 but not TCF12 gene during skeletal muscle development.

Discussion

In this study, we investigated the function and molecular mechanisms of miR-208b in skeletal muscle development. We provided novel evidence that miR-208b could elicit different functions by utilizing distinct mRNA targets in the same skeletal muscle tissue. miR-208b was originally identified in the MYH7 locus which encoded a myosin heavy chain beta isoform [17]. One previous study indicated that miR-208b could regulate cell cycle and promotes cattle primary myoblast cells proliferation by targeting CDKN1A [23]. In the current study, extensive in vivo and in vitro assays demonstrated that miR-208b not only stimulated the proliferation and inhibited differentiation of myogenic cells but also remodelled matured muscle into a slow fibre dominated, oxidative metabolism phenotype.

During myogenesis, miR-208b promoted proliferation and inhibited differentiation of myoblast mainly by repressing TCF12. TCF12 was involved in cellular proliferation and differentiation of different types of cells, including embryonic stem cells [23,24], CD4+/CD8 + T cells and bone marrow mesenchymal cells [25–28]. TCF12 could enhance the transcriptional activity of MyoD and MyoG [29]. Our Co-IP data provided a direct evidence of interactions among TCF12, MyoD, and MyoG. ChIP-seq data also confirmed that these three factors could bind at the same loci of the promoter regions of MyoD and MyoG. Therefore, TCF12, MyoD, and MyoG acted as complexes to positively regulate themselves during muscle development. Moreover, transcriptome analysis indicated that most of the differentially expressed genes of si-TCF12 and miR-208 overexpression treatments are overlapped. Thus, we concluded that TCF12 was the major target of miR-208b in myogenesis.

However, the energy metabolism genes and pathways enriched in miR-208b overexpression were not found in si-TCF12 treatment. Overexpression of TCF12 could not lead to the conversion of fast and slow myofibers. Therefore, we deduced that the other targets of miR-208b may mediate the energy metabolism of skeletal muscle.

In the current study, we confirmed that miR-208b could enhance energy metabolism and the slow muscle fibre programme via AMPK-PGC1a signalling pathway through targeting the FNIP1 gene both in vitro and in vivo. One previous study indicated that FNIP1 acted as an inhibitor of AMPK to repress energy metabolism [30]. FNIP1 was also reported to be targeted by miR-499 [19]. In this study, we also found that miR-499 has almost the same, yet a little weaker effect with miR-208b in C2C12 myotubes. Therefore, miR-208b and miR-499 may play overlapping roles in myogenesis and energy metabolism in skeletal muscle tissue. Further, it has been reported that miR-208a could inhibit whole-body energy metabolism through targeting MED13 gene [21]. Thus, we deduced that microRNAs encoded by myosin genes played different roles in energy metabolism through targeting different genes in skeletal muscle.

Taken together, our study established that miR-208b acted as a multi-functional switch during myogenesis, energy metabolism, and myofiber type conversion in skeletal muscle tissue. Therefore, the activities of miR-208b and its downstream signalling must be precisely tuned to meet the different requirements of varied tasks in skeletal muscle, and this could be achieved by the actions of miR-208b/TCF12 and miR-208b/FNIP1 pathways (Fig. 7).
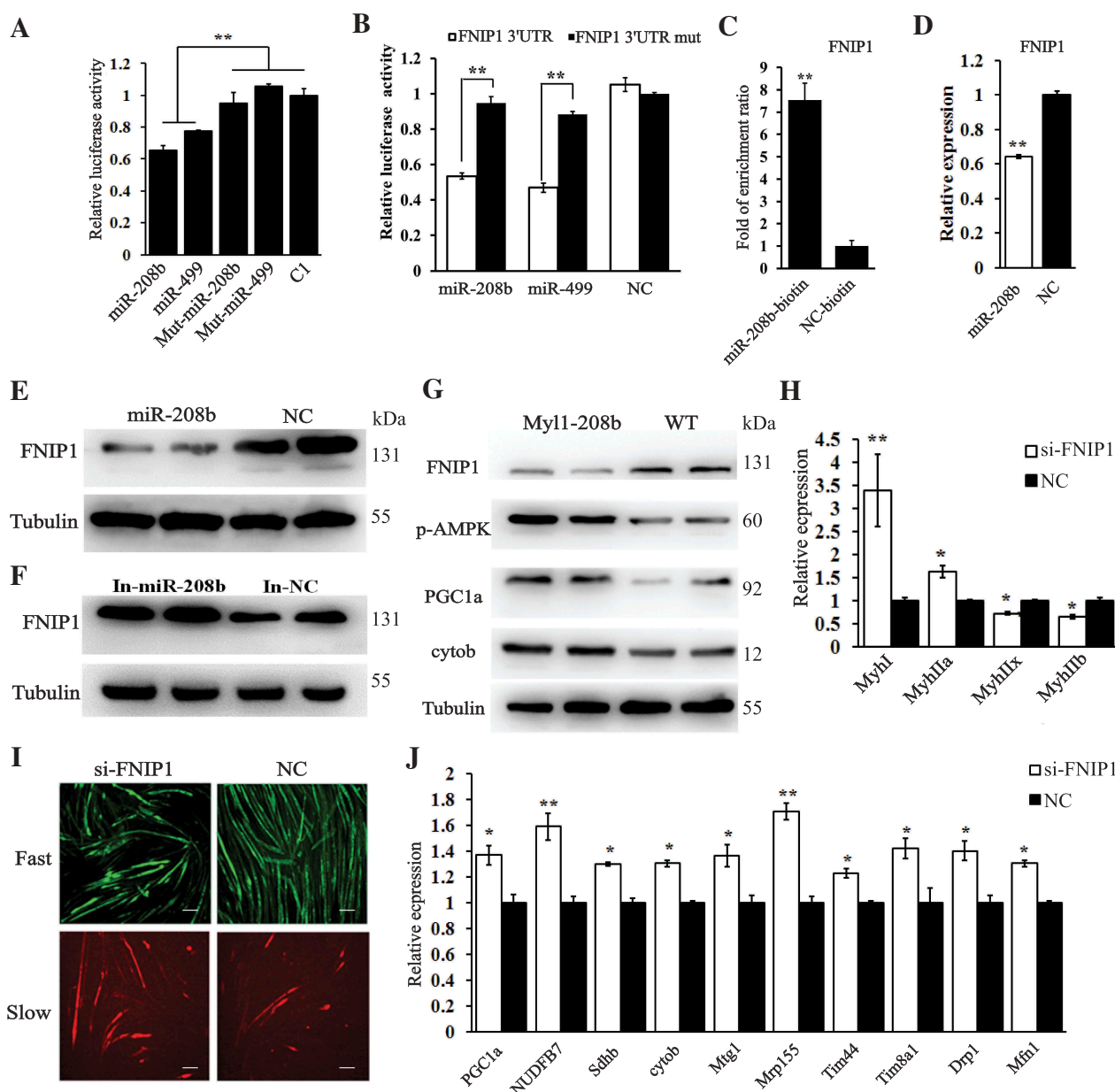
Figure 6. miR-208b regulates energy metabolism and fibre type conversion through targeting FNIP1 gene.

(A and B) The wild and mutant FNIP1 3' UTR were inserted into the dual-luciferase reporter vector psi-CHECK2 at the 3' end of the *Renilla* luciferase gene (*hRluc*). The constructs were co-transfected with pEGFP-miR-208b, pEGFP-mut-miR-208b, pEGFP-miR-499, pEGFP-mut-miR-499, or pEGFP-C1 (C1) into BHK-21 cells, and normalized *Renilla* luciferase activity was measured. (C) The miR-208b-biotin pull-down assays were performed and the PNIP1 mRNA level was detected by Q-PCR. (D) C2C12 myotubes were transfected with miR-208b or NC after transfection, the mRNA expression of FNIP1 was detected by Q-PCR. (E and F) C2C12 myotubes transfected with miR-208b mimic, NC, miR-208b inhibitor, or NC were differentiated for 48 h. FNIP1 protein expression was detected by Western blotting. (G) The leg muscle protein level of FNIP1, phosphor-AMPKα (Thr172), PGC1a, and Cytob was examined in WT and Myl1-208b mice at 2 months of age by Western blotting. (H-J) C2C12 myoblasts were induced into myotubes for 96 h after induction, and myotubes were transfected with si-FNIP1 or NC sequentially differentiated for 48 h. (H) The mRNA expression of MyHc-I, MyHc-IIa, MyHc-IIb, and MyHc-IIx genes was detected by Q-PCR. (I) Immunostaining of C2C12 myotubes was performed using myosin-fast and myosin-slow antibody. (J) The mRNA expression of mitochondrial energy metabolism genes (PGC1a, NUDFB7 Sdhb, Cytob, Mtg1, Mrp155, Timm44, TIm8a1, Drp1, and Mfn1) was detected by Q-PCR. The results are presented as mean ± SEM (n = 3). Tubulin mRNA was used as internal control for the expression of functional genes. *, P < 0.05; **, P < 0.01.

Material and methods

Animals

Myl1-cre mice were obtained from Jackson Laboratory (Bar Harbour, ME, USA). Loxp-miR-208b transgenic mice in a C57BL/6 background were generated by Cyagen Biosciences. Overexpression of miR-208b in TG mice was generated by breeding Loxp-miR-208b male mice with Myl1-cre female mice. Mice were housed and maintained in the animal facility with free access to standard rodent chow and water. All experiments were performed according to the Guide for the Care and Use of Laboratory Animals (Institute of Laboratory Animal Resources, Commission on Life Sciences, National Research Council, 1996). Leg muscle samples were collected from male
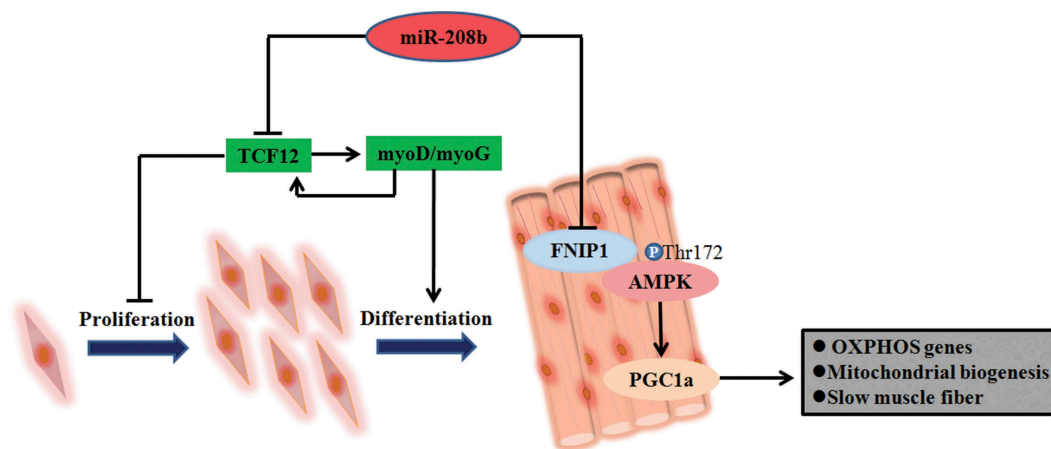
Figure 7. Model of miR-208b-mediated regulation of skeletal muscle development and homoeostasis.

C57 mice with 4 weeks and 8 weeks of age. Samples were frozen in liquid nitrogen and stored at −80°C until RNA and protein isolation.

Cells culture, transfection, and luciferase assay

The growth medium for C2C12 cells and BHK-21 cells was high-glucose Dulbecco's modified Eagle's medium (DMEM; Hyclone) and 10% foetal bovine serum (Gibco). For induction of myoblasts into myotubes, DMEM containing 3% horse serum (Gibco) was used. Cells were transfected using Lipofectamine 2000 (Invitrogen) according to the manufacturer's recommendations. miRNA mimics, mutants, and scrambled negative control were provided by RiboBio. The miRNA mimics were synthesized as duplexes. The miRNA sequences were: mmu-miR-208b: 5′-AUAAGACGAACAAAA GGUUUGU −3′, 3′- AAACCUUUUGUUCGUCUUAUUU-5′, mmu-miR-499-5P: 5′-UUAAGACUUGCAGUGAUGUU U-3′, 3′-ACAUCACUGCAAG UCUUAAUU-5′, mut-miR-20 8b:5′-AUAAGACUAACAAAAGGUUUGU-3′, 3′- AAACCU UUUGUUAGUCUUAUUU-5′, NC: 5′-UUCUCCGAACGUG UCA CGUTT-3′, 3′-ACGUGACACGUUCGGAGAATT-5′. Plasmid transfection into BHK-21 cells was performed using Lipofectamine 2000 at 24 h. After transfection, luciferase assay was performed with a Dual-Luciferase Reporter Assay System (Promega) according to the manufacturer's recommendations.

Western blotting

The skeletal muscle samples were first lysed with cold T-PER Tissue Protein Extraction Reagent (Thermo, USA). Cell samples were lysed with RIPA buffer (Sigma). Then, the protein concentration of the lysates was measured using the BCA protein kit (Beyotime, China). After that, proteins were sorted with SDS-polyacrylamide gel, and then transferred to polyvinylidene fluoride membranes (Millipore, USA). Then, the membranes were blocked with 5% non-fat milk in Tris-buffered saline containing 0.1% Tween-20 (TBST) for 1 h at room temperature. Subsequently, the membranes were incubated overnight at 4°C using primary antibodies against FNIP1 (Abcam, 1:1000 dilution), TCF12 (Santa Cruz Biotechnology, 1:200 dilution), MyoD (Santa Cruz Biotechnology, 1:200 dilution), MyoG (DSHB, 1:100 dilution), PGC1a (Abcam, 1:1000 dilution), AMPK (CST, 1:1000 dilution), phospho-AMPKα (Thr172) (Santa Cruz Biotechnology, 1:200 dilution), CYC (Santa Cruz Biotechnology, 1:200 dilution), and α-tubulin (Abcam, 1:1000 dilution). The HRP-labelled anti-rabbit/mouse IgG secondary antibody (Beyotime, China; 1:2000 dilution) was incubated for 1 h at room temperature. Finally, the protein bands were visualized using the Immobilon Western Chemiluminescent HRP substrate kit (Millipore, USA).

Quantitative PCR (Q-PCR)

Total RNA from mouse tissues and C2C12 cells was extracted using TRIzol reagent (Invitrogen, Carlsbad, CA, USA). Reverse transcription was performed using M-MLV reverse transcriptase (Invitrogen, USA). Q-PCR was carried out in a CFX384 Bio-Rad (Bio-Rad, USA) device using the SYBR Green PCR Master Mix kit (Toyobo, QPK201, Japan). Relative gene expression levels were calculated by $2^{-\Delta\Delta Ct}$ method. The levels of α-tubulin or GAPDH mRNA were used as internal control. T-test was conducted to analyse the statistical significance of differences. Significance level was set at $P < 0.05$. The sequence of the primers is presented in S5 Table.

Immunofluorescence

Fixed cells were incubated with anti-MyHc antibody (Santa Cruz Biotechnology, 1:200 dilution), anti-MYH7 antibody (Santa Cruz Biotechnology, 1:200 dilution), anti-fast skeletal muscle myosin antibody (Sigma, 1:500 dilution) as primary antibodies. Cells myotubes were then incubated with Alexa-Fluor-488-conjugated goat anti-mouse-Ig (H + L), Alexa-Fluor-555-conjugated goat anti-rabbit-IgG (H + L), or Alexa-Fluor-555-conjugated goat anti-mouse-IgG (H + L) (Invitrogen, USA) secondary antibodies. The cell nuclei were stained with DAPI. Images were captured using a Nikon ECLIPSE TE2000-S system.

Luciferase activity assay

The following primers were used to amplify the 3′ UTR fragments containing predicted miR-208b binding sites. TCF12 3′ UTR was amplified with the use of forward primer 5′-CTCGAGGTGTTTGCAGCATATCACTC-3′ and reverse primer 5′-GCGGCCGCTCTGCTTATCACTTCAAGGAC-3′. FNIP1 3′ UTR was amplified with the use of forward primer 5′-CTCGAGTCCAACCTGCTTCATTCCACT-3′ and reverse primer 5′-GCGGCCGCAGAGTGGGTGCTTGCTACCG. The restriction enzymes *Xho*I (NEB) and *Not*I (NEB) were used to insert these fragments into the psiCHECK-2 vector (Promega). To produce TCF12 and FNIP1 mutated plasmids, site-directed mutation was used to introduce 3 base substitution to the miR-208b binding site of psiCHECK-2 vector. A dual-luciferase reporter assay system (Promega) was used to analyse the relative luciferase activity [31].

Cell cycle flow cytometry

Twenty-four hours after transfection, C2C12 cells were fixed in 70% ethanol overnight at −20°C. Following incubation in 50 µg/mL propidium iodide solution (which contained 100 µg/mL RNase A and 0.2% (v/v) Triton X-100) for 30 min at 4°C. The cells were analysed using a FACSCalibur (Becton Dickinson, Franklin Lakes, NJ, USA) and the ModFit software (Verity Software House, Topsham, ME, USA). The proliferative index (PI) stands for the proportion of mitotic cells from a total of 20 000 cells examined.

Edu assay

Twenty-four hours after transfection with mimic-miR-208b, mut-miR-208b, or NC, C2C12 cells were cultured with fresh growth medium containing EdU (final concentration, 10 µM) for 2 h. Cells were fixed with 4% paraformaldehyde and permeabilized, and the cell nuclei were stained with DAPI. Images were captured using a Nikon ECLIPSE TE2000-S system.

Co-immunoprecipitation

TCF12-coding sequence was amplified by the forward primer 5′-ATGGATTACAAGGATGACGACGATAAG AATCCCCA GCAGCAGCGC-3′ and reverse primer 5′-CAGATGACCC ATAGGGTTGGT-3′, and inserted into pcDNA-3.1. MyoD-coding sequence was amplified by the forward primer5′-ATGTACCCATACGACG TCCCAGACTACGCTATGGAGC TTCTATCGCCGCCA-3′ and reverse primer 5′-TCAA AGCACCTGATAAATCGCA-3′, and inserted into pcDNA-3.1. Total protein was extracted from C2C12 cells transfected with pcDNA-FLAG-TCF12-3.1 or pcDNA-HA-MyoD-3.1. The lysate was pre-cleared with protein G beads at 4°C for 30 min. Then, 4 µg of primary antibody FLAG, HA, or mouse IgG (Santa Cruz Biotechnology) was added into cell lysate containing 500 mg total protein, and rotated at 4°C overnight. Protein G beads were added into cell lysate and rotating for overnight at 4°C. The samples were washed extensively 6 times and subjected to Western blot analysis.

ATP assay

The ATP assay kit was from Beyotime and the assay was performed according to the manufacturer's instruction. ATP amounts were normalized to protein and presented as percent relative to control.

Creatine kinase activity assay

Myotubes were washed 3 times with PBS and then lysed with lysis buffer. Whole-cell lysates were centrifuged for 15 min at 10,000 rpm, and the supernatant was stored at −80°C for the determination of creatine kinase (CK) activity. The CK activity was determined using a commercial kit (Nanjing Jiancheng Bioengineering Institute, China), following the manufacturer's protocol.

Biotinylated miRNA pull-down assays

C2C12 cells were transfected with 100 nM miR-208b-biotin mimic or NC mimics-biotin (Guangzhou RiboBio Co., Ltd). After 24 h transfection, the whole-cell lysates were collected, mixed with streptavidin beads (Invitrogen) and incubated overnight at 4°C. After washed thoroughly, the bead-bound RNA was isolated by TRIzol reagent and detected by Q-PCR. The mRNA levels of tubulin were used as an internal control of Q-PCR.

ChIP-seq

ChIP-seq data for MyoD and MyoG in MB and MT, TCF12 in MT were collected from ENCODE public repository. To unify the criteria for peak calling, aligned ChIP-seq reads for MyoD, MyoG, and TCF12 were fed to MACS (version 2.0.9), using the threshold of q-value <0.01 with the input ChIP-seq sample as the background. Other options were set as default.

RNA-seq and data analysis

Solexa sequencing was used to detect the differentially expressed gene. cDNA libraries were constructed using the TruSeq Stranded Total RNA LT Sample Prep kit (Illumina, Santiago, CA, USA). Library construction and solexa sequencing were performed by The Beijing Genomics Institute (Shenzhen, China). Raw RNA sequencing reads were mapped to the reference genome using Tophat. Transcripts were assembled, and expression levels were quantified to identify differentially expressed genes with Cufflinks and Cuffdiff. All the RNA-seq data in this study were submitted into the Sequence Read Archive (SRA) database (Accession NO. SRP241161).

Statistical analysis

All results are shown as the mean±s.e.m., and at least three independent individuals or replicates were used per group. Unpaired Student's *t*-tests were used to determine statistical significance, and $P < 0.05$ was considered significantly different.

Acknowledgments

Author Contributions

XL and SZ conceived this study. LF, HW., YL, and PZ performed the Two-dimensional electrophoresis, Immunofluorescence, Immunohistochemistry, Western blotting and Q-PCR experiments and prepared the materials involved in this study. LF., YX., and YZ contributed to data analysis. LF, SZ, and XL. drafted the manuscript. All authors read and approved the final manuscript.

Disclosure statement

No potential conflict of interest was reported by the authors.

Funding

References

[1] Janssen I, Heymsfield SB, Wang ZM, et al. Skeletal muscle mass and distribution in 468 men and women aged 18-88 yr. J Appl Physiol. 2000;89:81–88.

[2] Buckingham M, Bajard L, Chang T, et al. The formation of skeletal muscle: from somite to limb. J Anat. 2003;202:59–68.

[3] Bentzinger CF, Wang YX, Rudnicki MA. Building muscle: molecular regulation of myogenesis. Cold Spring Harb Perspect Biol. 2012;4:a008342-a008342.

[4] Koo JH, Kim TH, Park S-Y, et al. Gα13 ablation reprograms myofibers to oxidative phenotype and enhances whole-body metabolism. J Clin Invest. 2017;127:3845–3860.

[5] Meng ZX, Gong J, Chen Z, et al. Glucose sensing by skeletal myocytes couples nutrient signaling to systemic homeostasis. Mol Cell. 2017;66:332-+.

[6] Posner AD, Soslow JH, Burnette WB, et al. The correlation of skeletal and cardiac muscle dysfunction in duchenne muscular dystrophy. J Neuromuscul Dis. 2016;3:91–99.

[7] Gagan J, Dey BK, Layer R, et al. Notch3 and Mef2c proteins are mutually antagonistic via Mkp1 protein and miR-1/206 microRNAs in differentiating myoblasts. J Biol Chem. 2012;287:40360–40370.

[8] Zhang D, Wang X, Li Y, et al. Thyroid hormone regulates muscle fiber type conversion via miR-133a1. J Cell Biol. 2014;207:753–766.

[9] Wei W, He H-B, Zhang W-Y, et al. miR-29 targets Akt3 to reduce proliferation and facilitate differentiation of myoblasts in skeletal muscle development. Cell Death Dis. 2013;4:e668.

[10] Zeng P, Han W, Li C, et al. miR-378 attenuates muscle regeneration by delaying satellite cell activation and differentiation in mice. Acta Biochim Biophys Sin (Shanghai). 2016;48:833–839.

[11] Sato T, Yamamoto T, Sehara-Fujisawa A. miR-195/497 induce postnatal quiescence of skeletal muscle stem cells. Nat Commun. 2014;5:4597.

[12] Lee K-P, Shin YJ, Panda AC, et al. miR-431 promotes differentiation and regeneration of old skeletal muscle by targeting Smad4. Genes Dev. 2015;29:1605–1617.

[13] Dey BK, Gagan J, Dutta A. miR-206 and −486 induce myoblast differentiation by downregulating Pax7. Mol Cell Biol. 2011;31:203–214.

[14] Crippa S, Cassano M, Messina G, et al. miR669a and miR669q prevent skeletal muscle differentiation in postnatal cardiac progenitors. J Cell Biol. 2011;193:1197–1212.

[15] Shi L, Zhou B, Li P, et al. MicroRNA-128 targets myostatin at coding domain sequence to regulate myoblasts in skeletal muscle development. Cell Signal. 2015;27:1895–1904.

[16] Wei W, Zhang W-Y, Bai J-B, et al. The NF-kappa B-modulated microRNAs miR-195 and miR-497 inhibit myoblast proliferation by targeting Igf1r, Insr and cyclin genes. J Cell Sci. 2016;129:39–50.

[17] van Rooij E, Quiat D, Johnson BA, et al. A family of microRNAs encoded by myosin genes governs myosin expression and muscle performance. Dev Cell. 2009;17:662–673.

[18] Wang XG, Ono Y, Tan SC, et al. Prdm1a and miR-499 act sequentially to restrict Sox6 activity to the fast-twitch muscle lineage in the zebrafish embryo. Development. 2011;138:4399–4404.

[19] Liu J, Liang X, Zhou D, et al. Coupling of mitochondrial function and skeletal muscle fiber type by a miR-499/Fnip1/AMPK circuit. EMBO Mol Med. 2016;8:1212–1228.

[20] Gan Z, Rumsey J, Hazen BC, et al. Nuclear receptor/microRNA circuitry links muscle fiber type to energy metabolism. J Clin Invest. 2013;123:2564–2575.

[21] Grueter CE, van Rooij E, Johnson B, et al. A cardiac microRNA governs systemic energy homeostasis by regulation of MED13. Cell. 2012;149:671–683.

[22] Hu JS, Olson EN, Kingston RE. Heb, a helix-loop-helix protein related to E2a and Itf2 that can modulate the DNA-binding ability of myogenic regulatory factors. Mol Cell Biol. 1992;12:1031–1042.

[23] Yoon SJ, Foley JW, Baker JC. HEB associates with PRC2 and SMAD2/3 to regulate developmental fates. Nat Commun. 2015;6. ARTN 6546. DOI:10.1038/ncomms7546.

[24] Yoon SJ, Wills AE, Chuong E, et al. HEB and E2A function as SMAD/FOXH1 cofactors. Genes Dev. 2011;25:1654–1661.

[25] Wojciechowski J, Lai A, Kondo M, et al. E2A and HEB are required to block thymocyte proliferation prior to pre-TCR expression. J Immunol. 2007;178:5717–5726.

[26] Miyazaki M, Miyazaki K, Chen K, et al. The E-Id protein axis specifies adaptive lymphoid cell identity and suppresses thymic innate lymphoid cell development. Immunity. 2017;46:818.

[27] Yi SQ, Yu M, Yang S, et al. Tcf12, a member of basic helix-loop-helix transcription factors, mediates bone marrow mesenchymal stem cell osteogenic differentiation in vitro and in vivo. Stem Cells. 2017;35:386–397.

[28] Jones-Mason ME, Zhao X, Kappes D, et al. E protein transcription factors are required for the development of CD4+ lineage T cells. Immunity. 2012;36:348–361.

[29] Parker MH, Perry RL, Fauteux MC, et al. MyoD synergizes with the E-protein HEB beta to induce myogenic differentiation. Mol Cell Biol. 2006;26:5771–5783.

[30] Reyes NL, Banks GB, Tsang M, et al. Fnip1 regulates skeletal muscle fiber type specification, fatigue resistance, and susceptibility to muscular dystrophy. Proc Natl Acad Sci U S A. 2015;112:424–429.

[31] Feng Y, Niu -L-L, Wei W, et al. A feedback circuit between miR-133 and the ERK1/2 pathway involving an exquisite mechanism for regulating myoblast proliferation and differentiation. Cell Death Dis. 2013;4:ARTN e934.